Zak phases and band properties in acoustic metamaterials with negative modulus or negative density

Li Fan,* Wei-wei Yu, Shu-yi Zhang, Hui Zhang, and Jin Ding
Lab of Modern Acoustics, Institute of Acoustics, Nanjing University, Nanjing 210093, China
(Received 27 June 2016; revised manuscript received 31 October 2016; published 28 November 2016)

Zak phases in two types of acoustic metamaterials with negative density or negative modulus are studied. Different from phononic crystals based on Bragg scattering, extraordinary performance in acoustic metamaterials originates from local resonance. We find that the Zak phases in metamaterials are determined by the resonances of scatterers, side pipes, or membranes. Additionally, it is observed that the topological transition points, symmetrical properties of edge states, input impedances, and reflection phases in forbidden bands are all related to the resonances of the scatterers, and the relationship can be used to create surface states at the interface of two types of acoustic metamaterials.

DOI: 10.1103/PhysRevB.94.174307

The geometric phase, which is induced by the geometrical properties of the parameter space of the Hamiltonian, is a phase difference acquired over the course of a cycle while a system is subjected to cyclic adiabatic processes [1]. In addition to quantum mechanics, the studies concerning the geometric phase were spread into various wave systems [2–5]. Then the Zak phase, which specifically refers to the geometric phase that characterizes the topological energy bands of electron motions in one-dimensional periodic solids, was presented [6]. The Zak phase was first measured on the basis of a dimerized model [7] corresponding to the classical Su-Schrieffer-Heeger model devised to study soliton formation in polyacetylene [8,9]. Furthermore, the studies concerning the Zak phase were conducted in photonic crystals theoretically [10] and experimentally [11,12], and then interface states and band topology in two-dimensional photonic crystals were studied [13,14]. Recently, the concept of the Zak phase was introduced into acoustics [15], in which the Zak phases and interface states were measured in a phononic crystal composed of an alternately established cylindrical pipe with two types of cross-sectional areas.

Apart from phononic crystals, acoustic metamaterials are considered to be the other type of artificial materials which can produce unprecedented acoustic phenomena. The fundamental mechanisms for phononic crystals and acoustic metamaterials are completely different. For phononic crystals, Bragg scattering in periodic structures is the primary mechanism of band gaps [16]. From the perspective of acoustic transmission, the gaps are induced by the reflections of acoustic waves, which originate from the mismatch of acoustic impedances at the boundaries of the periodic structures in phononic crystals. Unlike phononic crystals, characteristic frequency bands and extraordinary performance of metamaterials result from local resonance of artificial structures other than Bragg scattering [17]. Therefore, in this work, we explore the relations between the Zak phase and local resonance of two types of scatterers, side pipes or membranes, in the acoustic metamaterial with a negative modulus or negative density, respectively. Furthermore, due to the local resonance, the band edges in the metamaterials are classified into two types induced by different mechanisms, which also determine the symmetrical properties of the edge states. Finally, on the basis of the relationship among the Zak phases, input impedances, and reflection phases, interface states are created at the border of two types of metamaterials with negative modulus or negative density.

The models of two types of metamaterials are shown in Fig. 1, in which the negative density is realized with periodically distributed membranes M_i [18,19] and the negative modulus is created by side pipes P_i with hard terminals other than side holes [19–21] or Helmholtz resonators [22]. In both metamaterials, the acoustic waves in adjacent units U_{N-1} and U_N can be expressed based on Bloch theory [19,21]:

$$\begin{bmatrix}\Pi_N^+\\ \Pi_N^-\end{bmatrix}=\mathbf{\Gamma}\begin{bmatrix}\Pi_{N-1}^+\\ \Pi_{N-1}^-\end{bmatrix}=\begin{bmatrix}\Gamma_{11} & \Gamma_{12}\\ \Gamma_{21} & \Gamma_{22}\end{bmatrix}\begin{bmatrix}\Pi_{N-1}^+\\ \Pi_{N-1}^-\end{bmatrix}, \tag{1}$$

where Π represents the acoustic pressure p or particle velocity v, and the superscripts $+$ and $-$ represent the incident and reflected waves, respectively. $\mathbf{\Gamma}$ is the transfer matrix indicating the relationship between the quantities Π in the adjacent units. Neglecting damping, the components of the transfer matrix for the negative-modulus metamaterial $\mathbf{\Gamma}_M$ can be obtained as $\Gamma_{M11}=(1+j\rho_0c_0/2SX_{HA})e^{-jkL}$, $\Gamma_{M12}=j\rho_0c_0/2SX_{HA}$ and $\Gamma_{M22}=\Gamma_{M11}^*$, $\Gamma_{M21}=\Gamma_{M12}^*$, where the asterisk indicates complex conjugation. $X_{HA}=-\rho_0c_0\tan^{-1}(kl_s)/S_s$ is the effective reactance of the side pipes determined by the effective length l_s and cross-sectional area $S_s=\pi r_s^2$ of the side pipes [23]. $S=\pi a^2$ is the cross-sectional area of the main tube, L is the length of the unit, and k is the wave number of the conventional acoustic waves. ρ_0 and c_0 are the density and acoustic velocity of air in the metamaterial, respectively. Then, solving the eigenequation (1), we can obtain the eigenvalues $\lambda_M^{\pm}=e^{\pm jq_ML}$ and corresponding eigenvectors $\mathbf{B}_M=[\beta_1,\beta_2]^T=[\Gamma_{M12},e^{jq_ML}-\Gamma_{M11}]^T$, where the superscript T indicates transposition. Furthermore, the dispersion equation and eigenvectors can be achieved:

$$\cos(q_ML)=\cos(kL)+\sin(kL)\rho_0c_0/2SX_{HA}, \tag{2}$$

and

$$\mathbf{B}_M=[j\rho_0c_0/2SX_{HA},j\{\sin(q_ML)+\sin(kL)-\cos(kL)\rho_0c_0/2SX_{HA}\}]^T, \tag{3}$$

*fanli@nju.edu.cn

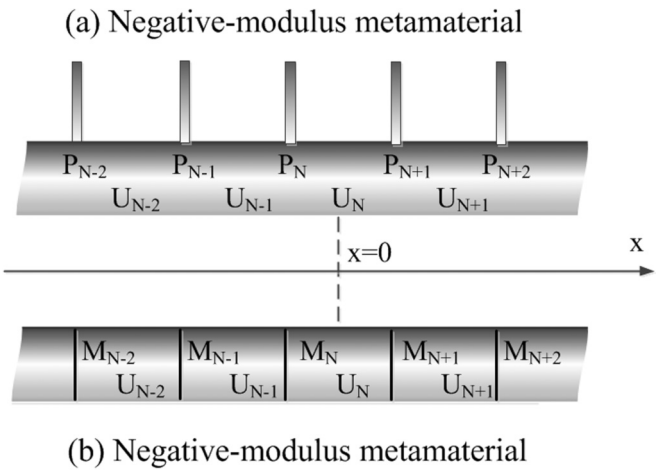

FIG. 1. Models of the metamaterials with (a) negative modulus and (b) negative density.

where q_M is the Bloch wave number for the negative-modulus metamaterial.

For plane acoustic waves transmitting along the x direction, the Zak phase for the mth isolated passband is defined to be [15]

$$\theta_m^{\mathrm{Zak}} = \int_{-\pi/L}^{\pi/L} \left[j \int_{\text{unit cell}} \frac{1}{2\rho_0 c_0^2} dx \Pi_{m,q_M}^*(x) \partial_{q_M} \Pi_{m,q_M}(x) \right] \times dq_M. \quad (4)$$

The system is invariant under space inversion if the inversion center is chosen at the origin $x = 0$, and thus the distribution of the Bloch wave exhibits a space symmetry of $\Pi_{m,q_M}(x) = \Pi_{m,-q_M}(-x)$. Therefore, the Zak phase calculated with Eq. (4) must be 0 unless the isolated passband contains a special frequency f_{Ar} at which both β_1 and β_2 equal 0. From Eq. (3), β_1 and β_2 simultaneously equal 0 at the frequency where $X_{HA} \to \infty$ (see Supplemental Material, Part I [24]), which demonstrates that f_{Ar} is the antiresonance frequency of the side pipes [23]. In this case, the coefficient matrix $\mathbf{\Gamma}$ exhibits a diagonal form, and we do not need to search for the eigenvectors. Therefore, in the passbands containing the antiresonance frequencies f_{Ar}, the system acquires a Zak phase of π; otherwise the Zak phase is 0. Furthermore, for the metamaterial with a negative density, it can be proven that if an isolated passband covers a resonant frequency f_{Mr} of the membranes, at which the effective reactance of the membrane $X_{MA} = 0$, the Zak phase of the band is π; otherwise the Zak phase is 0 (see Supplemental Material, Part I [24]). Thus it is demonstrated that the local resonance of the scatterers determines the Zak phase in an acoustic metamaterial.

According to the Zak phases, the isolated passbands in acoustic metamaterials can be classified into two types, which exhibit different properties in band edges and symmetry of eigenstates. First, we can determine the band edges in the negative-modulus metamaterial from dispersion Eq. (2). Defining a dimensionless normalized acoustic impedance $Z_M = \rho_0 c_0 / 2SX_{HA}$, Eq. (2) can be rewritten as $\cos(q_M L) = \sqrt{1 + Z_M^2} \cos(kL - \alpha_M)$, where $\tan(\alpha_M) = Z_M$, from which the band edges can be determined by $kL = m\pi$ or $kL - 2\alpha_M = m\pi$ ($m = 1,2,3,\ldots$). Different from phononic crystals in which the Bragg resonance is a sole reason for band gaps, the metamaterial exhibits two types of band edges resulting from different mechanisms: $kL = m\pi$ (type I) indicates the band edges induced by the Bragg resonance, which is solely determined by the unit length L and independent of the parameters of the scatterers, while the band edges characterized by $kL - 2\alpha_M = m\pi$ (type II) are determined by the impedance of the side pipes. The local resonance frequencies f_r of the side pipes must locate in forbidden bands, because at f_r, we have $X_{HA} = 0$ [23], which results in $Z_M \to \infty$ and $|\cos(q_M L)| > 1$. Then the passbands must locate between local resonant frequencies of the side pipes and do not contain f_r. On the other hand, the antiresonance frequencies f_{Ar} of the side pipes must locate in passbands since $Z_M = 0$ at f_{Ar}. Thus, as shown in Fig. 2(a), we classify the passbands into two types; one does not cover an antiresonance frequency f_{Ar} [PB1 and PB2], and the other, induced by the antiresonance, contains f_{Ar} (PB3). For the former, if $Z_M < 0$, namely, $\alpha_M \in (-\pi/2,0)$ (as PB1), the bottom edge is type I and the top edge is type II. When $Z_M > 0$ and $\alpha_M \in (0,\pi/2)$ (as PB2), the bottom edge is type II and the top edge is type I. In the antiresonance induced passband (as PB3), we have $Z_M > 0$ at the bottom edge and $Z_M < 0$ at the top edge, and both edges must be type II. Besides, the origin of the frequency axis $f = 0$ can also be considered to be an antiresonant frequency, and thus the top edge of the first passband is type II.

Due to the occurrence of two types of band edges, the widths of pass and/or forbidden bands in an acoustic metamaterial can differ massively. Provided that L is sufficiently small and no band edge of type I induced by Bragg scattering occurs between adjacent f_r and f_{Ar}, one achieves an extremely wide passband with the Zak phase of π covering the majority of the frequency range between two adjacent f_r. Furthermore, when an antiresonant frequency f_{Ar} of the side pipe is in accordance with a Bragg-resonance frequency of the metamaterial, namely, $Z_M = 0$ and $kL = m\pi$ are simultaneously achieved at f_{Ar}, two passbands cross each other and the forbidden band between them closes, as indicated in the middle panel of Fig. 2(b). Then, by tuning the structural parameters across the passband crossing point f_{Ar}, the Zak phases of the passbands on both sides of f_{Ar} switch between 0 and π, which demonstrates that f_{Ar} is a topological transition point (see Supplemental Material, Part II [24]). In addition, two adjacent forbidden bands can also degenerate into one if a local resonant frequency f_r and a Bragg-resonance frequency are in agreement with each other, and thus a simple band structure can be obtained, as shown in the bottom panel in Fig. 2(b).

The eigenstates of band edges obtained at the inversion center are related to the local resonance of the scatterers. At the origin $x = 0$ of the coordinates, which is an inversion center in space, the acoustic pressure in the negative-modulus metamaterial can be expressed to be $p_0 = T_{M12} + (e^{jq_M L} - T_{M11})$, and meanwhile, at band edges, we have $e^{jq_M L} - T_{M11} = \pm T_{M12}$. Thus the amplitude of acoustic pressure $|P_A|$ at $x = 0$ only has two values, zero or the maximum, corresponding to the edge states of antisymmetry and symmetry, respectively. Similar results can be obtained in the particle velocity, in which the antisymmetrical and symmetrical states are opposite to those of the acoustic pressure.

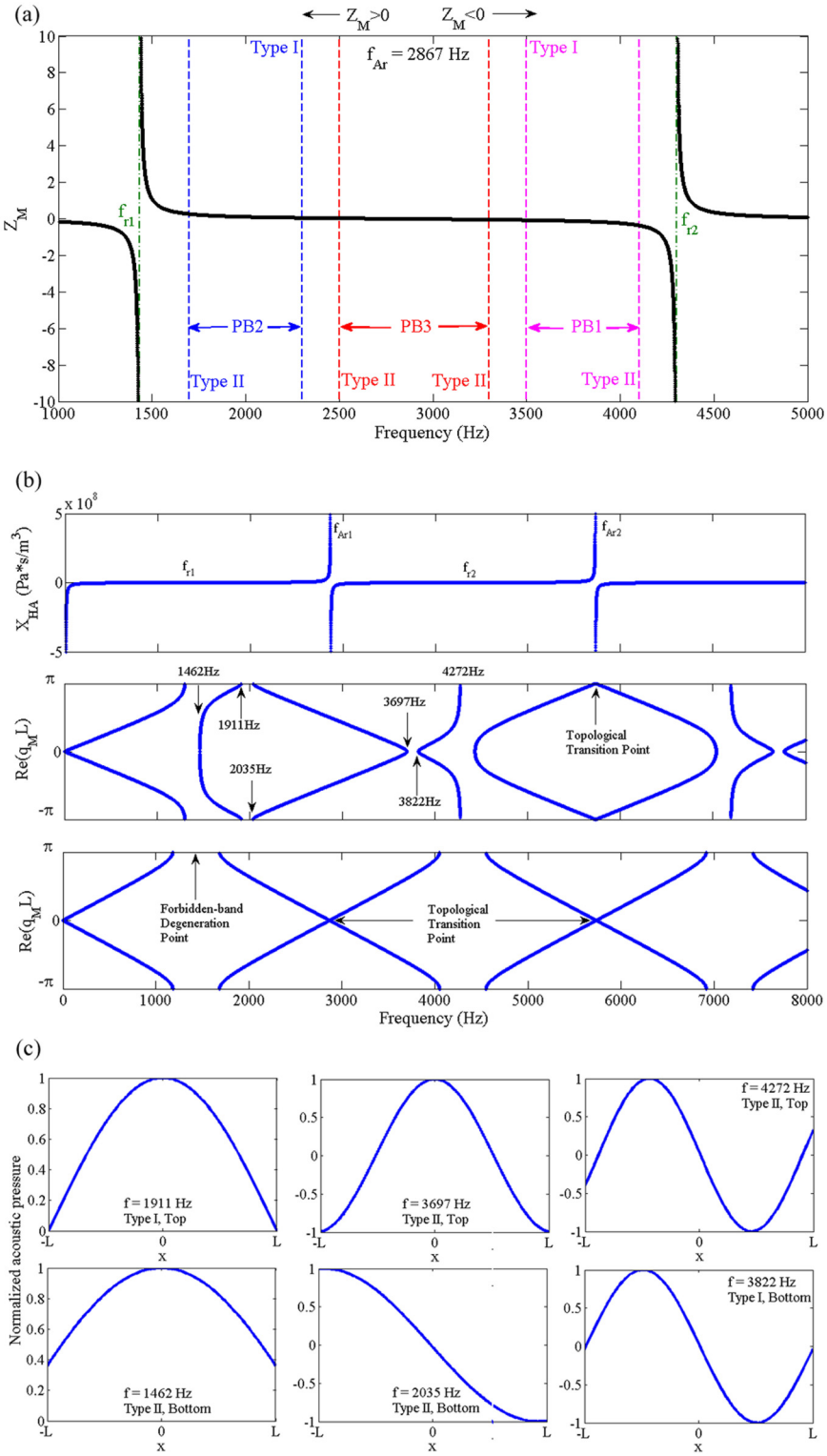

FIG. 2. (a) Classification of the bands and band edges between two adjacent resonant frequencies f_{r1} and f_{r2} of the side pipes. (b) The reactance X_{HA} of the side pipes (upper panel) calculated with $l_s = 6$ cm and $r_s = 1$ cm, and the band structures with $L = 9$ cm (middle panel) and $L = 12$ cm (bottom panel). The cross-sectional radius of the main waveguides is $a = 2.5$ cm. It can be observed that with $L = 12$ cm, both the passbands and forbidden bands degenerate, which produces a simple band structure. (c) Symmetrical characteristics of the band edges at the inversion center obtained in three passbands between f_{r1} and f_{r2} indicated in the middle panel of (b). In the PB1-type passband between 3822 Hz ($m = 2$) and 4272 Hz($m' = 3$), the edge states for the top and bottom edges obtained at $x = 0$ are both zero and exhibit antisymmetrical characteristics. In the PB2-type passband between 1462 Hz ($m = 0$) and 1911 Hz ($m' = 1$), both edge states reach the maximum and show symmetrical properties. In the PB3-type passband between 2035 Hz ($m = 1$) and 3697 Hz ($m = 1$), the eigenstate at the bottom edge is zero and that at the top edge reaches the maximum, which demonstrate different symmetrical characteristics.

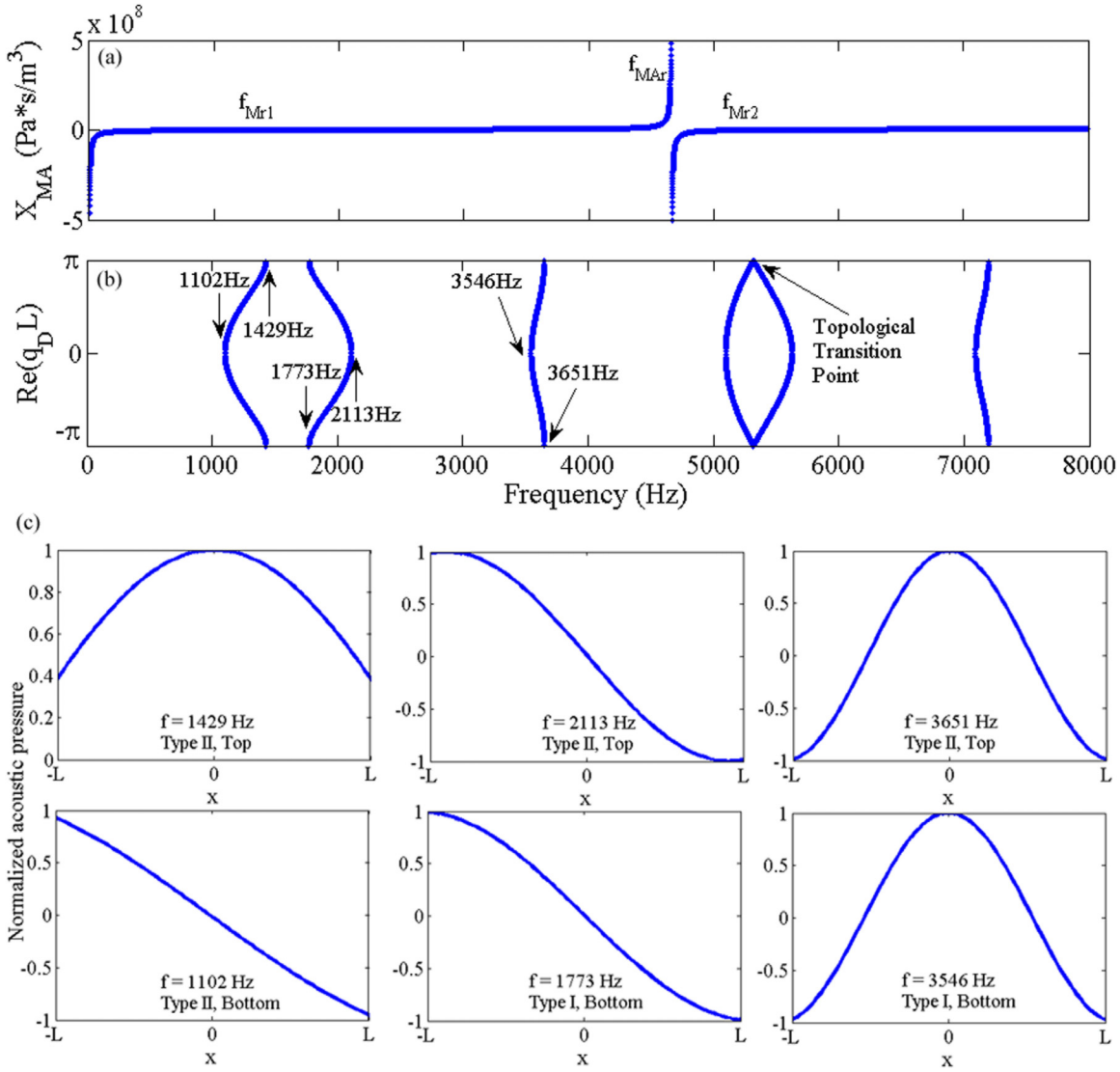

FIG. 3. (a) The reactance X_{MA} of the membranes calculated with the following parameters: a mass of $m_M = 0.35$ g, a thickness of $t = 125\,\mu$m, a radius of $a = 2.5$ cm, a Young's modulus $E = 2.66 \times 10^{11}$ N/m^2, and a Poisson's ratio of $\upsilon = 0.34$. (b) Band structure of the negative-density metamaterial with $L = 9.7$ cm. (c) Symmetrical characteristics of the band edges in the first three passbands shown in (b) obtained at the inversion center. For the passband between 1102 and 1429 Hz, which is a resonance induced passband covering a resonant frequency of the membrane and exhibits the Zak phase of π, both band edges are type II and show different eigenstates. For the passbands of $1773 - 2113$ Hz and $3546 - 3651$ Hz, with the Zak phases of 0, the bottom edges are type I and the top edges are type II, which exhibit the same eigenstates.

For a PB1-type passband ($Z_M < 0$), the bottom and top edges are, respectively, determined by $kL = m\pi$ and $kL - 2\alpha_M = m'\pi$, with $m' = m + 1$. When m is even, $|P_A|$ at bottom and top edges are both zero, and when m is odd, they reach the maximum, which indicate that the edge states for the top and bottom edges are the same. For a PB2-type passband ($Z_M > 0$), both edge states are also the same. However, in an antiresonance induced passband like PB3, regardless of m, the amplitudes of acoustic pressures $|P_A|$ are different at the bottom and top edges. Thus it is demonstrated that the edge states for both edges are opposite to each other in an isolated passband with the Zak phase of π, while they are the same in a passband with the Zak phase of 0. The detailed explications are presented in the Supplemental Material, Part III [24]. Furthermore, the calculated space distributions of the acoustic pressures at the band edges are shown in Fig. 2(c), which demonstrate the symmetrical characteristics of the band edges previously predicted based on the classification of band edges.

The characteristics for the band structure and eigenstates in the negative-density metamaterial are shown in Fig. 3. Comparing Figs. 2 and 3 shows that although the reactances X_{HA} and X_{MA} are similar in both types of scatterers, the band structures in the metamaterials are different. For the negative-density metamaterial, the membranes, exhibiting high impedance at low frequencies, are established in series along the main waveguide, which causes intensive impedance mismatch and creates a forbidden band in the low-frequency range. While in the negative-modulus metamaterial, the side pipes, which also exhibit high impedances at low frequencies,

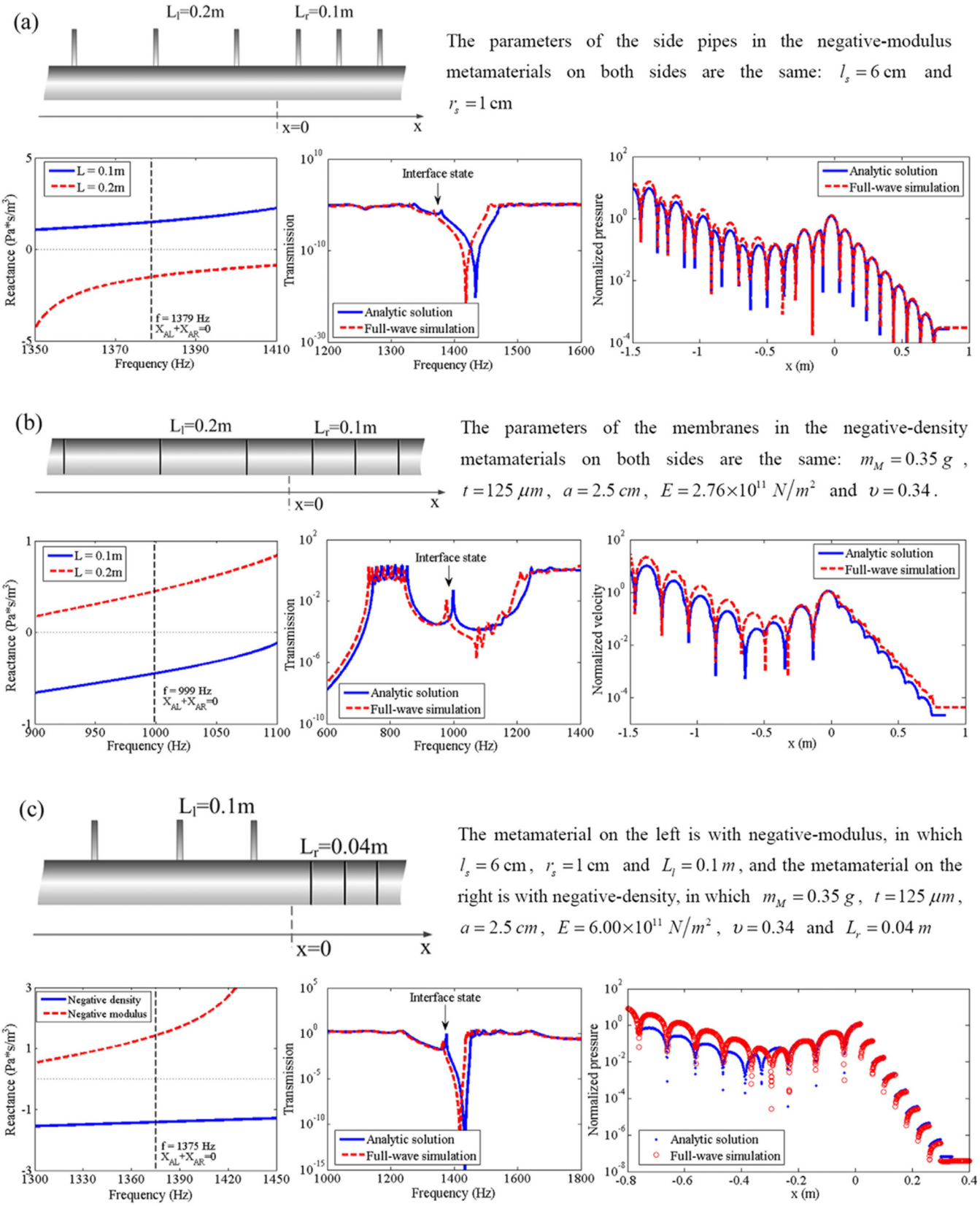

FIG. 4. Input reactances, transmissions, and space distributions of the acoustic pressures in three types of composite structures.

are established in parallel and laterally along the main waveguide. Thus, in the low-frequency range, the side pipes exert a marginal impact on the acoustic transmission, which result in a passband. Due to the high impedance of the membrane at the antiresonant frequencies, the passbands in the negative-density metamaterial locate between antiresonant frequencies and do not contain them. As shown in Fig. 3, the classification of band edges and symmetrical properties of edge states are similar to those in the negative-modulus metamaterial, and details can be found in the Supplemental Material, Part III [24].

The input impedances Z_{in} in forbidden bands of the acoustic metamaterials are also related to the local resonance and the Zak phases. Assuming a plane acoustic wave is normally incident to the negative-modulus metamaterial at $x = 0$, the relationship between the reflection coefficient $R = |R|e^{j\varphi_R}$ and the input impedance Z_{in} is

$$\frac{1+R}{1-R} = Z_{\text{in}} = \rho_0 c_0 \frac{\xi^+ - j}{\xi^- + j}, \tag{5}$$

in which $\zeta^{\pm} = [\text{Im}(T_{M12}) \pm \text{Im}(e^{jq_M L} - T_{M11})]/[(-1)^{n+1}2\sinh(\kappa)]$. In a forbidden band, we have $e^{jq_M L} = \pm e^{-\kappa}$, with $\kappa > 0$ indicating the decay in acoustic transmission. n indicates the number of times that the value of the dispersion equation $\cos(q_M L)$ changes between $\cos(q_M L) < -1$ and $\cos(q_M L) > -1$. After some derivations (see Supplemental Material, Part IV [24]), the sign of the reflection phase in the zth forbidden band can be obtained as $\text{sgn}[(1+R)/(1-R)] = \text{sgn}(\varphi_R) = \text{sgn}(X_{\text{in}}) = (-1)^{z+s+s'+1}$, where s is the number of the antiresonant frequency f_{Ar} which is not a topological transition point and s' is the number of forbidden-band degeneration points below the zth forbidden band. It can be observed that if two forbidden bands degenerate, the reflection phase exhibits opposite signs on both sides of the degeneration point inside the degenerated forbidden band.

Moreover, in the negative-density metamaterial, the signs of the reflection phase and input reactance are opposite to those in the negative-modulus metamaterial with the same z, s, and s' (see Supplemental Material, Part IV [24]).

Then, according to the reflection phase and input impedance, an interface state can be created on the basis of structures composed of two metamaterials, as indicated in Fig. 4. When the input reactances X_{AL} and X_{AR} of the metamaterials on the left and right sides satisfy the relation of $X_{AL} + X_{AR} = 0$ [10,15], an interface state can be achieved at $x = 0$. Therefore, if the forbidden bands in the metamaterials on both sides overlap and the input reactances or reflection phases are opposite in sign, it provides a possibility to form an interface state. The left panel in Fig. 4(a) shows the input reactances in the forbidden bands of two negative-modulus metamaterials obtained with the impedance transfer theory, which indicate that the condition $X_{AL} + X_{AR} = 0$ is obtained at 1379 Hz. Moreover, the frequency-domain response and spatial distribution of the acoustic pressure in the composed structure are calculated using the theory describing the acoustic transmission in periodic structures. From the transmission shown in Fig. 4(a), we can observe a peak at 1379 Hz, although this frequency locates in the forbidden bands of both metamaterials. Meanwhile, the space distribution of the acoustic pressure at 1379 Hz is displayed in the right panel, which exhibits a peak at the interface $x = 0$, indicating an interface state; although in a forbidden band, the acoustic pressure should decay along the structure from the input at the left terminal to the right end. To verify the results obtained with the analytic theory, COMSOL MULTIPHYSICS is used to carry out full-wave simulations. As shown in Fig. 4(a), the results of the full-wave simulations are in accordance to those obtained with the analytic theory. Furthermore, interface states are also created in the structures composed of two negative-density metamaterials and even different types of metamaterials, as indicated in Figs. 4(b) and 4(c), respectively, which demonstrates that an interface state can be achieved provided that the condition $Z_{AL} + Z_{AR} = 0$ is satisfied, regardless of the types of the metamaterials composing the structure. Additionally, it has been proven that the damping in a system exerts no influences on the band structure [25,26], and thus the Zak phase in the metamaterials is independent of the damping. However, the loss dissipates the acoustic energy in the metamaterial, which can decrease the amplitudes of the interface states [15].

In conclusion, it is demonstrated that the Zak phase in an isolated passband of an acoustic metamaterial is primarily determined by the local resonance. Meanwhile, due to the local resonance, the band edges in acoustic metamaterials are classified into two types induced by different mechanisms. Additionally, the local resonance in the metamaterials also determines the topological transition points, forbidden-band degeneration points, band-edge states, input impedances, and reflections in forbidden bands. Therefore, on the basis of the relationship between the Zak phases and the signs of the input impedances, an interface state can be created in a structure composed of two metamaterials. Furthermore, based on the analogy between acoustic, optic, and electromagnetic metamaterials, the research in this work can also be spread into optic or electromagnetic metamaterials.

This work is supported by the National Basic Research Program of China Grant No. 2012CB921504; National Natural Science Foundation of China, Grants No. 11374154, No. 10904067, No. 11174142, and No. 11274169; Natural Science Foundation of Jiangsu Province of China Grant No. BK20151375; and Special Fund for Research in Quality Inspection of Public Welfare Industry, Grant No. 201510068.

[1] M. V. Berry, Proc. R. Soc. London, Ser. A **392**, 45 (1984).
[2] S. Ryu and Y. Hatsugai, Phys. Rev. B **73**, 245115 (2006).
[3] M. Pechal, S. Berger, A. A. Abdumalikov, Jr., J. M. Fink, J. A. Mlynek, L. Steffen, A. Wallraff, and S. Filipp, Phys. Rev. Lett. **108**, 170401 (2012).
[4] I. G. Ryabinkin and A. F. Izmaylov, Phys. Rev. Lett. **111**, 220406 (2013).
[5] I. Yulevich, E. Maguid, N. Shitrit, D. Veksler, V. Kleiner, and E. Hasman, Phys. Rev. Lett. **115**, 205501 (2015).
[6] J. Zak, Phys. Rev. Lett. **62**, 2747 (1989).

[7] M. Atala, M. Aidelsburger, J. T. Barreiro, D. Abanin, T. Kitagawa, E. Demler, and I. Bloch, Nat. Phys. **9**, 795 (2013).
[8] W. P. Su, J. R. Schrieffer, and A. J. Heeger, Phys. Rev. Lett. **42**, 1698 (1979).
[9] V. Dal Lago, M. Atala, and L. E. F. Foa Torres, Phys. Rev. A **92**, 023624 (2015).
[10] M. Xiao, Z. Q. Zhang, and C. T. Chan, Phys. Rev. X **4**, 021017 (2014).
[11] W. S. Gao, M. Xiao, C. T. Chan, and W. Y. Tam, Opt. Lett. **40**, 5259 (2015).
[12] Q. Wang, M. Xiao, H. Liu, S. N. Zhu, and C. T. Chan, Phys. Rev. B **93**, 041415 (2016).
[13] D. A. Abanin, T. Kitagawa, I. Bloch, and E. Demler, Phys. Rev. Lett. **110**, 165304 (2013).
[14] X. Q. Huang, Y. T. Yang, Z. H. Hang, Z. Q. Zhang, and C. T. Chan, Phys. Rev. B **93**, 085415 (2016).
[15] M. Xiao, G. C. Ma, Z. Y. Yang, P. Sheng, Z. Q. Zhang, and C. T. Chan, Nat. Phys. **11**, 240 (2015).
[16] J. T. Barreiro, Nat. Phys. **11**, 215 (2015).
[17] Z. Y. Liu, X. X Zhang, Y. W. Mao, Y. Y. Zhu, Z. Y. Yang, C. T. Chan, and P. Sheng, Scinece **289**, 1734 (2000).
[18] S. H. Lee, C. M. Park, Y. M. Seo, Z. G. Wang, and C. K. Kim, Phys. Lett. A **373**, 4464 (2009).
[19] L. Fan, Z. Chen, Y. C. Deng, J. Ding, H. Ge, S. Y. Zhang, Y. T. Yang, and H. Zhang, Appl. Phys. Lett. **105**, 041904 (2014).
[20] S. H. Lee, C. M. Park, Y. M. Seo, Z. G. Wang, and C. K. Kim, J. Phys.: Condens. Matter. **21**, 175704 (2009).
[21] L. Fan, H. Ge, S. Y. Zhang, H. F. Gao, Y. H. Liu, and H. Zhang, J. Acoust. Soc. Am. **133**, 3846 (2013).
[22] N. Fang, D. J. Xi, J. Y. Xu, M. Ambati, W. Srituravanich, C. Sun, and X. Zhang, Nat. Mater. **5**, 452 (2006).
[23] L. E. Kinsler, A. R. Frey, A. B. Coppens, and J. V. Sanders, *Fundamentals of Acoustics* (Wiley, New York, 1982).
[24] See Supplemental Material at http://link.aps.org/supplemental/10.1103/PhysRevB.94.174307 for details of the derivations in the main text.
[25] F. Bongard, H. Lissek, and J. R. Mosig, Phys. Rev. B **82**, 094306 (2010).
[26] C. E. Bradley, J. Acoust. Soc. Am. **96**, 1844 (1994).